

## Reduction of Rocksalt Phase in Ag-Doped $\text{Ge}_2\text{Sb}_2\text{Te}_5$ : A Potential Material for Reversible Near-Infrared Window

Palwinder Singh,<sup>1,2</sup> A.P. Singh,<sup>3</sup> Jeewan Sharma,<sup>4</sup> Akshay Kumar,<sup>4</sup> Monu Mishra,<sup>5</sup> Govind Gupta,<sup>5</sup> and Anup Thakur<sup>2,\*</sup>


<sup>1</sup>*Department of Physics, Punjabi University, Patiala, Punjab 147002, India*

<sup>2</sup>*Advanced Materials Research Lab, Department of Basic and Applied Sciences, Punjabi University, Patiala, Punjab 147002, India*

<sup>3</sup>*Department of Physics, Dr. B. R. Ambedkar National Institute of Technology, Jalandhar 144011, India*

<sup>4</sup>*Department of Nanotechnology, Sri Guru Granth Sahib World University, Fatehgarh Sahib, Punjab 140407, India*

<sup>5</sup>*Advanced Materials and Devices Division, CSIR-National Physical Laboratory, New Delhi 110012, India*

 (Received 15 July 2018; revised manuscript received 1 November 2018; published 30 November 2018)

Phase-change materials are attracting much attention in the scientific and engineering communities owing to their applications and underlying basic phenomena.  $\text{Ge}_2\text{Sb}_2\text{Te}_5$  is reversible-phase-change material (amorphous to crystalline and vice versa) that is used for optical data storage and phase-change random-access memory and has recently been explored for use as a reversible near-infrared (NIR) window [Singh *et al.*, Appl. Phys. Lett. 111, 261102 (2017)]. For a reversible NIR window, large transmission contrast between two phases and low phase-transition temperature are required to reduce the power consumption. In the present work, phase transition in thermally deposited  $(\text{Ge}_2\text{Sb}_2\text{Te}_5)_{100-x}\text{Ag}_x$  ( $x = 0, 1, 3, 5,$  and  $10$ ) thin films is achieved by vacuum thermal annealing. Transmission sharply decreases with phase transition in the NIR region.  $\text{Ge}_2\text{Sb}_2\text{Te}_5$  shows large transmission contrast (more than 50%) in the wavelength range from 1600 to 3200 nm with phase transition from an amorphous to a hexagonal-close-packed structure at 260 °C. In  $(\text{Ge}_2\text{Sb}_2\text{Te}_5)_{90}\text{Ag}_{10}$  thin films, a similar transmission contrast is achieved at a comparatively lower temperature (160 °C) due to reduction of the rocksalt phase. Distortion of the host lattice with addition of 10% Ag is confirmed from the drastic change in the density of states in the valence band and the shift in core-level ( $3d$ ) spectra of Ag, Sb, and Te. This distortion enables a hexagonal-close-packed phase in  $(\text{Ge}_2\text{Sb}_2\text{Te}_5)_{90}\text{Ag}_{10}$  thin films to be obtained at 160 °C.  $(\text{Ge}_2\text{Sb}_2\text{Te}_5)_{90}\text{Ag}_{10}$  could be a potential candidate for a reversible NIR window as it requires less power to achieve phase transition and high transmission contrast.

DOI: [10.1103/PhysRevApplied.10.054070](https://doi.org/10.1103/PhysRevApplied.10.054070)

### I. INTRODUCTION

In the modern era, materials exhibiting different structures in different conditions have unique importance from an application point of view. Phase-change materials (PCMs), based on a structural transition [1–6], are potential candidates for thermal storage [7], drug delivery [8], data storage [1,9], image recording [10,11], near-infrared (NIR) transmission [12], etc.

PCMs based on chalcogenides are aspiring candidates for data storage, transmission windows, and phase-change random-access memories [1,9,12].  $\text{GeTe}$ ,  $\text{Sb}_2\text{Te}_3$ ,  $\text{Ag-In-Sb-Te}$ ,  $\text{GeSb}_2\text{Te}_4$ ,  $\text{GeSb}_4\text{Te}_7$ , and  $\text{Ge}_2\text{Sb}_2\text{Te}_5$  are widely explored chalcogenide-based PCMs that exhibit the phenomenon of amorphous-to-crystalline phase transition

and vice versa.  $\text{Ge}_2\text{Sb}_2\text{Te}_5$  (GST) is a potential candidate for phase-transition technology due to its capability of phase transition on annealing, current/voltage pulse, and pressure owing to versatile properties such as fast crystallization speed, high thermal stability, and good data retention. GST has been mostly used for its optical and electrical contrast [13], and finds applications in optical data storage [9], phase-change random-access memory [13], and display devices [11].

Recently, there have been efforts to improve the properties of GST thin films in reference to thermal stability, crystallization speed, and phase-transition temperature by addition of different elements. The thermal stability and crystallization speed of GST were significantly increased by doping with Sn [14]. The activation energy of crystallization decreased with the addition of Si [15]. Carbon doping in GST enhanced the structural stability of both the

\*[dranupthakur@gmail.com](mailto:dranupthakur@gmail.com)

amorphous phase and the face-centered-cubic (fcc) phase by increasing the stressed rigid character of the material [16]. Carbon-doped GST is a promising material for low-power PCM applications because of its high resistivity and low thermal conductivity, which enable lower reset power compared with GST [16]. Irrespective of the preparation of samples, Ag addition is reported to significantly increase the speed of phase transition in GST thin films [17–20].

Many researchers are also interested in suppressing the rocksalt phase or the hexagonal-close-packed (hcp) phase of GST by doping it with an appropriate element to make it a potential candidate in various applications. The suppression of these phases of GST was reported by various researchers using different doping materials [21–27]. Seo *et al.* [21] found that addition of 10% Al to  $\text{Ge}_2\text{Sb}_2\text{Te}_5$  served as a center for the suppression of fcc-to-hcp transition, which led to a single-step crystallization process (i.e., amorphous to fcc phase). Similarly, addition of nitrogen [22–25], oxygen [26], or selenium [27] to GST played a role in suppressing the fcc phase and led to direct transition from the amorphous phase to the hcp phase. Jeong *et al.* [22] studied the effect of nitrogen addition from 2 to 31 at.% and suggested that addition of 31 at.% nitrogen in GST thin films leads to the hcp phase. This suggested that nitrogen dopant atoms enter the tetrahedral interstitial sites in the fcc crystal structure of the film and lead to distortion of the crystal structure, which in turn generates a strain field in the crystal lattice and is responsible for suppressing the fcc structure. Kim *et al.* [23] found a similar result with nitrogen addition and achieved direct hcp phase with nitrogen addition at 12 sccm. This suggested that the nitrogen atoms occupy either vacancies or tetrahedral interstitial sites, causing a shift in the characteristic peaks and increase of the lattice parameter. Direct phase transition to the hcp phase was also verified with nitrogen implantation [24,25]. A nitrogen implantation dose higher than  $4.51 \times 10^{16} \text{ cm}^{-2}$  resulted in direct transition from the amorphous phase to the hcp phase, with suppression of the fcc phase [24]. Jang *et al.* [26] observed direct phase transition with oxygen content above 16.7% in GST thin films. Vinod *et al.* [27] observed that  $\text{GST}_{1-x}\text{Se}_x$  ( $x = 0.00, 0.02, 0.10, 0.20, \text{ and } 0.50$  at.%) phase-change thin films crystallize directly to the stable hexagonal structure for  $x \geq 0.10$  when annealed at a temperature above 150 °C.

In the present study, we achieve phase transition from the amorphous phase to the hcp phase at a comparatively lower temperature with greater Ag addition ( $x \geq 5$ ) in GST thin films along with the rocksalt phase. A reversible NIR window is proposed at lower temperature.

## II. EXPERIMENTAL DETAILS

$(\text{Ge}_2\text{Sb}_2\text{Te}_5)_{100-x}\text{Ag}_x$  ( $x = 0, 1, 3, 5, \text{ and } 10$ ) bulk alloys are prepared by a melt quenching technique [28] from highly pure (99.999%) constituent elements (Ge, Sb,

Te, and Ag). Thin films of these alloys are deposited on glass substrates by a thermal-evaporation (Hind High Vacuum-BC-300) technique [28]. The thickness of the films is measured *in situ* by a digital thickness monitor (Hind High Vacuum DTM-101). The thickness of all deposited thin films is kept at approximately 700 nm. Films are annealed at 160 and 260 °C in a vacuum (approximately  $10^{-3}$  mbar) for 2 h.

Structural properties of as-deposited and annealed thin films are studied by an x-ray-diffraction (XRD) technique using an x-ray diffractometer (X'Pert PRO PANalytical) with Cu  $K_\alpha$  radiation ( $\lambda = 1.5406 \text{ \AA}$ ). The morphology of as-deposited and annealed thin films is studied with a JEOL JSM-6510 LV scanning electron microscope. Transmission spectra of as-deposited and annealed thin films are recorded at normal incidence with a UV-visible-NIR spectrophotometer (PerkinElmer Lambda 750) in the range from 800 to 3200 nm. Valence-band (VB) and core-level (Sb 3d, Te 3d, and Ag 3d) spectra of prepared samples are measured with an Omicron multiprobe surface analyzer (Scienta Omicron, Germany). A Mg  $K_\alpha$  radiation source (1253.6 eV) and a seven-channel detector are used for x-ray-photoelectron-spectroscopy data acquisition. The surface contaminants are removed by means of a mild sputtering method using 500 eV  $\text{Ar}^+$  ions for 10 min.

## III. RESULTS AND DISCUSSION

Figures 1(a)–1(e) show the XRD patterns of as-deposited and annealed  $(\text{Ge}_2\text{Sb}_2\text{Te}_5)_{100-x}\text{Ag}_x$  ( $x = 0, 1, 3, 5, \text{ and } 10$ ) thin films. There is no sharp peak in the XRD patterns (shown in black) of as-deposited thin films, which confirms the amorphous nature of all as-deposited films. The XRD pattern of GST thin film annealed at 160 °C confirms the rocksalt structure [29–31]. It is a metastable phase in which one lattice point is occupied by a Te atom and the other lattice point is occupied by either Ge or Sb or vacancies. The metastable phase consists of two well-defined three-dimensional repeating units: -Te-Ge-Te-Sb-Te- (I) and -Te-Sb-Te-Ge- (II) [32]. There are approximately 20% vacancies in this phase [33], and these play a vital role in the transition from the amorphous phase to the rocksalt phase [34,35]. There is significant local electronic change within GST crystallites that is mediated by vacancy ordering [36–38]. GST annealed at 260 °C has a hcp phase as confirmed by the XRD pattern [30,31]. The phase transition from the rocksalt structure to hcp is due to the movement of unit II in the [210] direction [32].

At both 160 and 260 °C, thin films with addition of 1% and 3% Ag have structures similar as those of GST films. Films with higher Ag content (5% and 10%) show a mixture of rocksalt and hcp phases on annealing at 160 °C and have a hcp phase at 260 °C. In thin films of GST doped with 5% Ag annealed at 160 °C, the rocksalt phase dominates, whereas in films of GST doped with 10% Ag, the

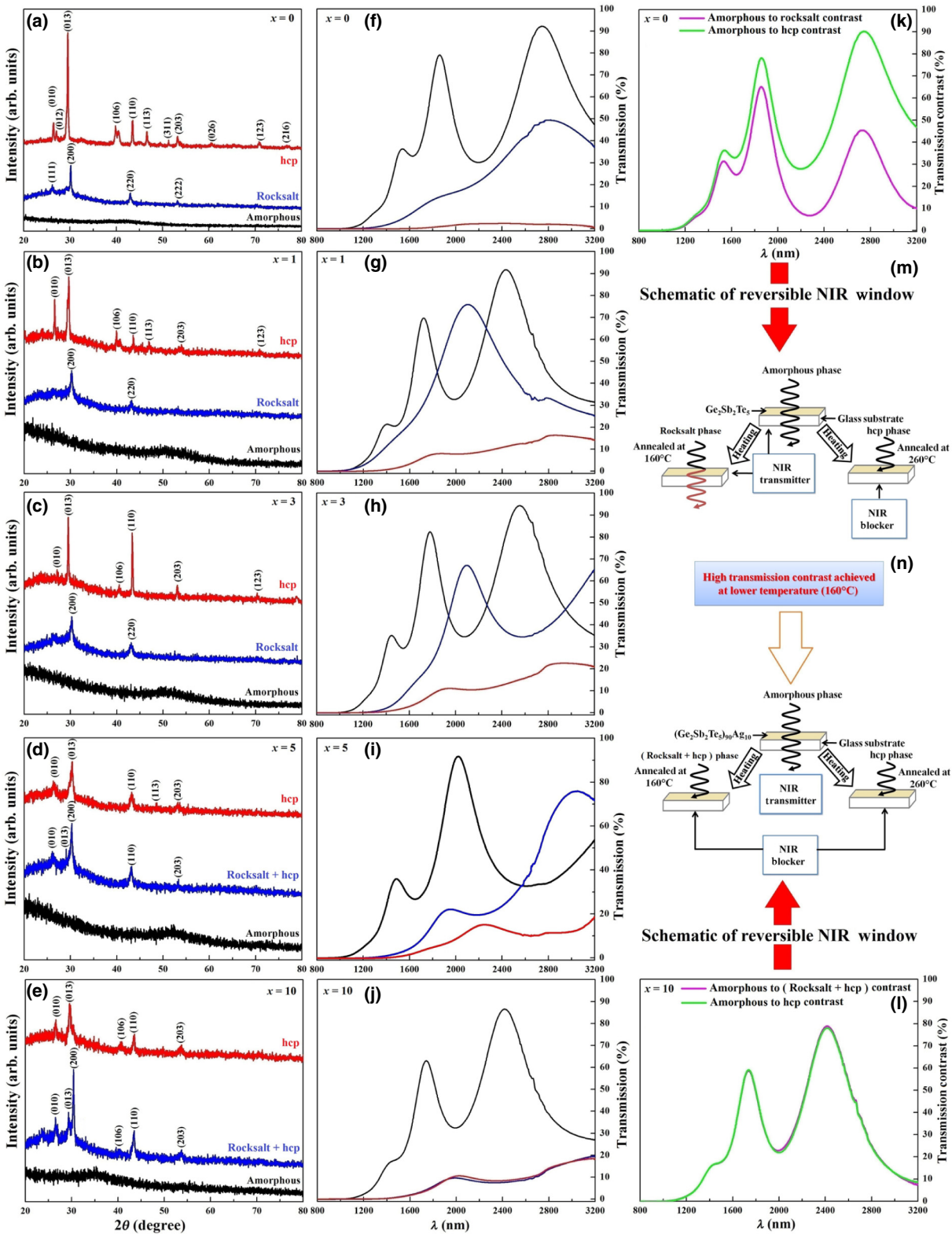


FIG. 1. As-deposited (black) and annealed (blue, 160 °C; red, 260 °C)  $(\text{Ge}_2\text{Sb}_2\text{Te}_5)_{100-x}\text{Ag}_x$  ( $x = 0, 1, 3, 5, \text{ and } 10$ ) thin films. (a)–(e) XRD patterns and (f)–(j) transmission spectra. (k),(l) Transmission contrast of  $(\text{Ge}_2\text{Sb}_2\text{Te}_5)_{100-x}\text{Ag}_x$  ( $x = 0$  and  $10$ ) between amorphous to rocksalt and amorphous to hcp phases. (m),(n) Reversible NIR window.

hcp phase dominates. These results suggest that higher Ag content (5% and 10%) helps to achieve the hcp structure at lower annealing temperature along with the rocksalt phase. This is a significant result in phase-change technology as the hcp phase is achieved at a lower temperature than reported by others [16,30–32].

The transmission spectra of as-deposited and annealed (160 and 260 °C)  $(\text{Ge}_2\text{Sb}_2\text{Te}_5)_{100-x}\text{Ag}_x$  ( $x = 0, 1, 3, 5,$  and  $10$ ) thin films are shown in Figs. 1(f)–1(j). It is clear from the spectra that all as-deposited thin films (black spectra) are highly transparent in the NIR region. Chalcogenide alloys are highly transparent beyond  $1 \mu\text{m}$  as these materials have high atomic masses and generate low-energy phonons in the amorphous network, conferring wide optical transparency extending far into the NIR region. The effect of Ag content on the optical transmission is also clear from Figs. 1(g)–1(j). The optical transmission increases with Ag addition up to 3% and starts decreasing afterward [39]. There is a large change in transmission in the NIR region on phase transition. In addition, the absorption edge is shifted toward higher wavelength with phase transition. It is also found that the absorption edge of Ag-doped thin films annealed at 160 °C approaches that of thin films annealed at 260 °C with higher Ag content (5% and 10%). For 10% Ag doping, the transmission spectra of films annealed at 160 and 260 °C almost overlap, which also confirms the similar structure at both temperatures. From these measurements, a considerable decrease in the transmission can be observed with the increase in the hcp phase. This decrease in transmission after phase transition is because of the presence of resonant  $p$  states in the crystalline phase, which are absent in the amorphous phase [40].

There is interest in making chalcogenide alloys applicable for transmission windows, lenses, and fibers beyond a wavelength of  $2 \mu\text{m}$  because of their limited visible transparency, low optical attenuation, large refractive index, high optical nonlinearity, and stability toward the atmosphere. The optical transmission windows of chalcogenide alloys are limited due to electronic absorption, Rayleigh scattering, and multiphonon absorption at short, intermediate and long wavelengths, respectively [41]. In addition, there are other losses present, such as a weak absorption tail and extrinsic losses. Some Te-based chalcogenide alloys explored for use as transmission windows include Ge-Se-Te, Ge-As-Se-Te, and As-Se-Te [41]. The shorter wavelength of the transmission window in amorphous chalcogenides is governed by their optical band gap. Incident light with energy higher than the optical band gap excites electron-hole pairs and is absorbed in the process. In these alloys, recombination of electron-hole pairs occurs in multiple nonradiative steps as they have negligible probability of photoluminescence.

The transmission contrast in the NIR region between the amorphous phase and the crystalline phase and the

rapid reversibility of Ge-Sb-Te alloys [42] can be used to design a reversible NIR transmission window [12]. It is clear from Figs. 1(f)–1(j) that  $(\text{Ge}_2\text{Sb}_2\text{Te}_5)_{100-x}\text{Ag}_x$  ( $x = 0, 1,$  and  $3$ ) thin films have large, medium, and negligible transmission in the NIR region for amorphous, rocksalt, and hcp phases, respectively.  $(\text{Ge}_2\text{Sb}_2\text{Te}_5)_{95}\text{Ag}_5$  thin film annealed at 160 °C has medium transmission as the rocksalt phase dominates over the hcp phase. On the other hand,  $(\text{Ge}_2\text{Sb}_2\text{Te}_5)_{90}\text{Ag}_{10}$  thin film annealed at 160 °C has negligible transmission as the hcp phase dominates. The transmission contrast for GST thin film and thin film of GST doped with 10% Ag from the amorphous phase to the rocksalt phase and from the amorphous phase to the hcp phase is shown in Figs. 1(k) and 1(l), respectively. The amorphous-to-hcp transmission contrast has a significant value, which is technologically important. GST has one drawback that this contrast is achieved at higher temperature (260 °C). On the other hand, comparable contrast is achieved at lower temperature (160 °C) in  $(\text{Ge}_2\text{Sb}_2\text{Te}_5)_{90}\text{Ag}_{10}$  thin films as shown in Fig. 1(l). Figures 1(m) and 1(n) show schematics depicting application of GST-based thin films as a reversible NIR window.

Ge-Sb-Te alloys are commercially used for optical data storage, where optical reflectivity contrast between the amorphous phase and the rocksalt phase is utilized [9]. Sun *et al.* reported the highest optical reflectivity (25%) contrast from the amorphous phase to the complete crystalline phase using femtosecond-laser irradiation [43]. In optical memory devices, data recording is done by writing an amorphous state on a crystalline film by local melting with a short pulse of focused and high-intensity laser light [9,13]. Rapid cooling of the melt, at rates higher than  $10^9$  K/s, results in an amorphous state. Data reading is done with a low-intensity laser beam as the amorphous state has lower reflectivity than the crystalline background. The erasing of the state is achieved by heating the amorphous state to a temperature above the glass transition temperature and allowing it to crystallize [9,13]. In a similar way, a reversible NIR window can be designed.  $(\text{Ge}_2\text{Sb}_2\text{Te}_5)_{90}\text{Ag}_{10}$  thin film is a potential material for a NIR window as it has large (negligible) transmission in the amorphous (crystalline) phase.

The optical transmission and reflection of thin films are dependent on the surface morphology [44]. The morphology of as-deposited  $(\text{Ge}_2\text{Sb}_2\text{Te}_5)_{100-x}\text{Ag}_x$  ( $x = 0, 3,$  and  $10$ ) thin films and annealed at different temperatures (160 and 260 °C) is shown in Fig. 2. The morphology of as-deposited thin films is smooth and uniform, which indicates the absence of crystallites, further confirming the amorphous nature of the films. No change in the morphology of as-deposited films is observed with Ag addition. The growth of crystallites can be visualized in the annealed thin films [45]. The effect of Ag addition on the morphology of the annealed thin films is observed. In annealed thin films, with addition of 3% Ag there is formation of



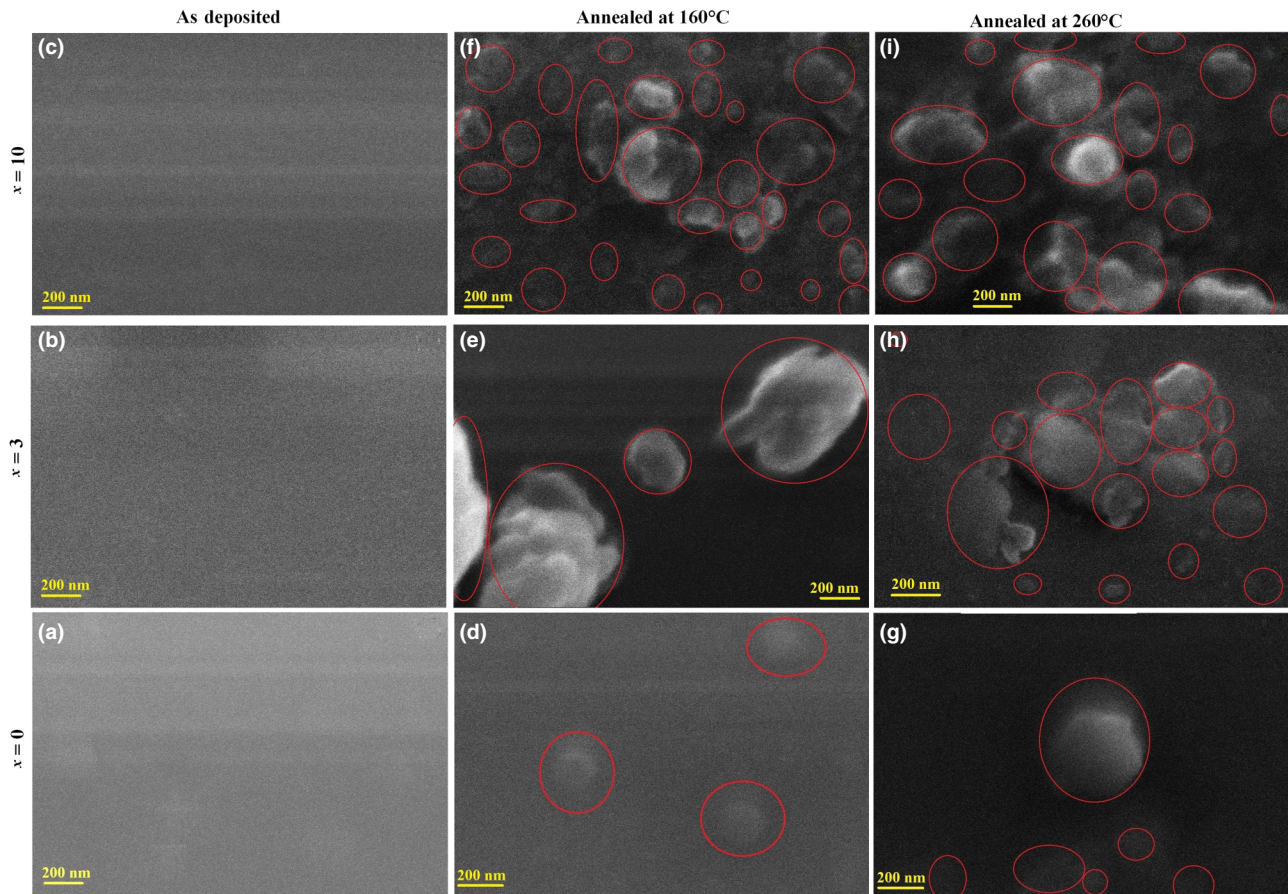


FIG. 2. (a)–(i) Scanning-electron-microscope images of as-deposited and annealed (at different temperatures)  $(\text{Ge}_2\text{Sb}_2\text{Te}_5)_{100-x}\text{Ag}_x$  ( $x = 0, 3,$  and  $10$ ) thin films.

larger grains or clusters as compared with GST thin films at the respective temperatures. A drastic change in the morphology with higher Ag content (10%) is observed with annealing. It is also observed that thin films doped with 10% Ag annealed at 160 and 260 °C have similar morphology. It can be inferred that Ag enhances nucleation and growth of crystallites in GST thin films.

To understand the role of Ag incorporation in GST thin films, X-ray photoelectron spectroscopy was performed. The core-level and VB spectra of  $(\text{Ge}_2\text{Sb}_2\text{Te}_5)_{100-x}\text{Ag}_x$  ( $x = 0, 3,$  and  $10$ ) thin films is studied. Figures 3(a)–3(c) show the core-level spectra of Ag (3d), Sb (3d), and Te (3d), respectively. It can be seen that the Ag (3d) core level shifts toward lower binding energy (BE), which indicates bonding of Ag with elements of GST. A shift of 0.4 and 1.1 eV in the BE of thin films with 3% and 10% Ag, respectively, is observed from Ag (3d) core-level spectra. It is highly unlikely that Ag will occupy the interstitial sites because of its larger size. The larger shift in the Ag (3d) spectrum of GST doped with 10% Ag suggests that there is more distortion in the lattice [28]. A shift is also observed in the Sb (3d) core-level spectra shown in Fig. 3(b). Figure 3(c) shows the core-level spectra of Te

(3d) of as-deposited thin films. Shifts of 0.5, 0.9, and 1.7 eV in the BE of Te (3d) core-level spectra are observed from the pure-metallic BE (573 eV). This shift in the spectra with Ag addition also confirms the bonding of Ag. The effect of Ag incorporation can be understood from the change in the density of states in VB spectra. Figure 3(d) shows the VB spectra of as-deposited thin films. The valence configurations are  $4s^24p^2$ ,  $5s^25p^3$ ,  $5s^25p^4$ , and  $4d^{10}5s^1$  for Ge, Sb, Te, and Ag, respectively. The VB spectra can be divided into two main parts [46]: region A (green shaded) near the valence-band maxima from about 0 to 6 eV, and region B (red shaded) from 6 to 14 eV. Region A contains the  $p$  bands of Ge  $4p$ , Sb  $5p$ , and Te  $5p$ , while region B is due to Ge  $4s$ , Sb  $5s$ , and Te  $5s$ . A significant change in the density of the valence state is observed with 10% Ag. The VB spectra of GST thin film and thin film of GST doped with 3% Ag are similar in shape but an additional feature around 1.5 eV appears with Ag addition. The VB spectrum of thin film of GST doped with 10% Ag is totally different from that of GST thin film and that of thin film of GST doped with 3% Ag, which may be due to the distortion in the host lattice [28]. An additional feature appears in thin film of GST doped with 3%

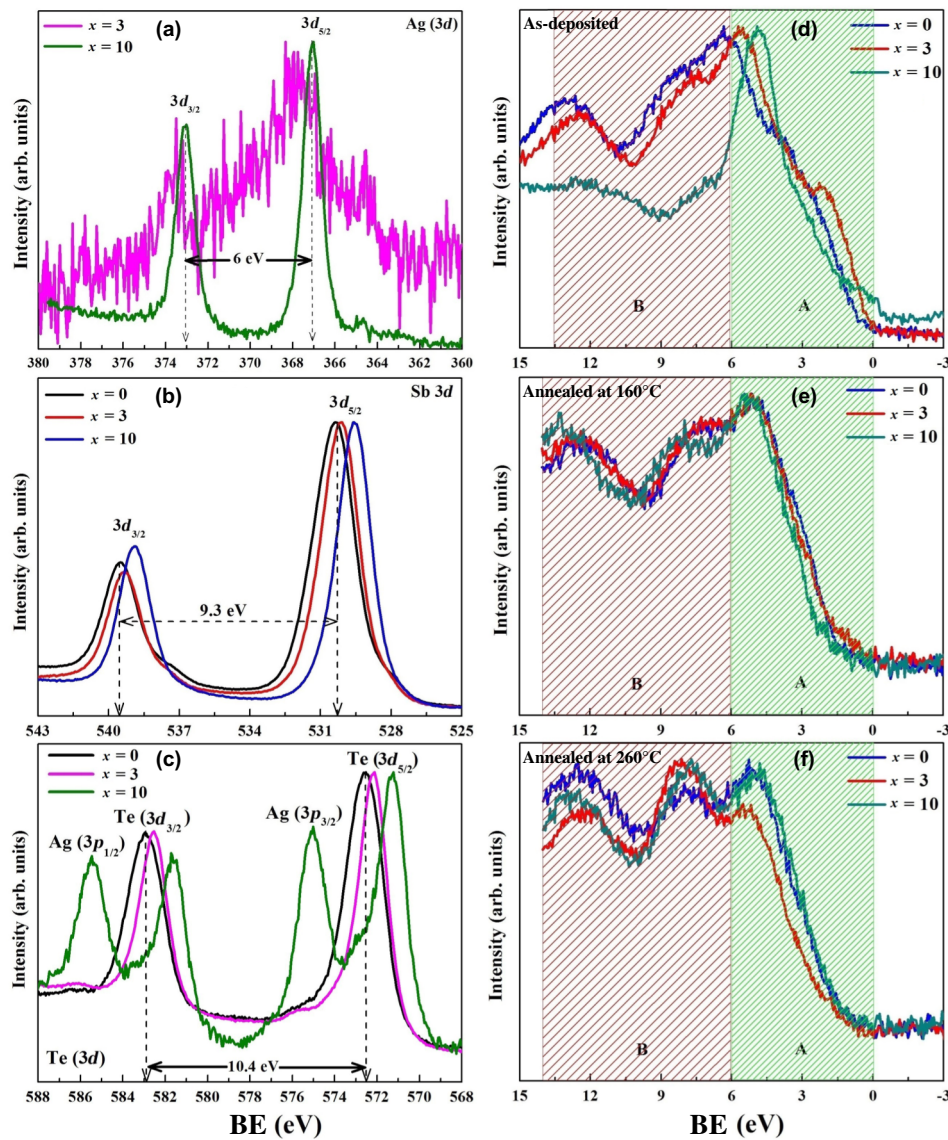


FIG. 3. Core-level spectra of as-deposited  $(\text{Ge}_2\text{Sb}_2\text{Te}_5)_{100-x}\text{Ag}_x$  ( $x = 0, 3$ , and  $10$ ) thin films: (a) Ag ( $3d$ ), (b) Sb ( $3d$ ), and (c) Te ( $3d$ ). Valence-band spectra of  $(\text{Ge}_2\text{Sb}_2\text{Te}_5)_{100-x}\text{Ag}_x$  ( $x = 0, 3$ , and  $10$ ) thin films: (d) as-deposited, (e) annealed at  $160^\circ\text{C}$ , and (f) annealed at  $260^\circ\text{C}$ .

Ag, and is shifted toward the Fermi level in thin film of GST doped with 10% Ag. All resolved features in region *B* disappear in thin film of GST doped with 10% Ag, and a single well-resolved peak around 5 eV is observed.

The VB spectra of the thin films annealed at 160 and  $260^\circ\text{C}$  are given in Figs. 3(e) and 3(f), respectively. The VB spectra of annealed samples are significantly different from those of the as-deposited samples. The crystalline samples show a steeper increase in intensity near the valence-band maxima with change in binding energy, which may be due to the higher absorption coefficient [47]. On the other hand, the change in intensity for the as-deposited sample is slightly less steep and a more-extended tailing off into the band-gap region is observed.

The broadening of spectral features for the amorphous spectra is because of atomic disorder. The VB spectra of the annealed films have almost the same shape, different from the as-deposited film, indicating change in the density of valence-band states on phase transition. The VB spectra of thin films of GST doped with 10% Ag annealed at 160 and  $260^\circ\text{C}$  have shape (as shown in Fig. 4) similar to that of GST annealed at  $260^\circ\text{C}$ , which also confirms the same electronic environment.

It is clear from core-level spectra of Ag, Sb, and Te that addition of a higher amount of Ag in GST results in a distorted host lattice and enables  $(\text{Ge}_2\text{Sb}_2\text{Te}_5)_{90}\text{Ag}_{10}$  to change its structural and optical properties as those of GST in hcp phase. It is important, from a technological



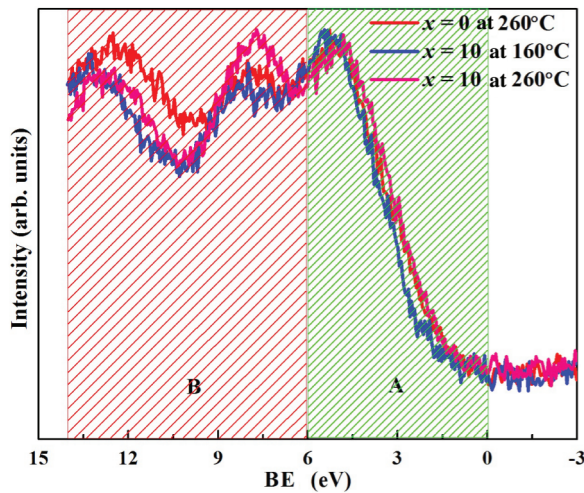


FIG. 4. Valence-band spectra of  $(\text{Ge}_2\text{Sb}_2\text{Te}_5)_{100-x}\text{Ag}_x$  thin films:  $x = 0$  annealed at  $260^\circ\text{C}$  and  $x = 10$  annealed at  $160$  and  $260^\circ\text{C}$ .

point of view, to achieve properties of the hcp phase at lower temperature as it is a stable phase of GST. Owing to optical transmission contrast on phase transition from the amorphous phase to the hcp phase and vice versa,  $(\text{Ge}_2\text{Sb}_2\text{Te}_5)_{90}\text{Ag}_{10}$  is a potential candidate for a reversible NIR window.

#### IV. CONCLUSION

The role of Ag addition in GST thin films is investigated. We explore rocksalt-phase reduction with higher Ag content.  $(\text{Ge}_2\text{Sb}_2\text{Te}_5)_{95}\text{Ag}_5$  thin films annealed at  $160^\circ\text{C}$  have a major rocksalt phase and a minor hcp phase, whereas  $(\text{Ge}_2\text{Sb}_2\text{Te}_5)_{90}\text{Ag}_{10}$  thin films have a major hcp phase and a minor rocksalt phase. This is also evident from optical transmission and x-ray-photoelectron-spectroscopy results. These results suggest the budding application of  $(\text{Ge}_2\text{Sb}_2\text{Te}_5)_{90}\text{Ag}_{10}$  thin film in reversible NIR windows.

[1] M. Wuttig, H. Bhaskaran, and T. Taubner, Phase-change materials for non-volatile photonic applications, *Nat. Photonics* **11**, 465 (2017).  
 [2] K. Ogata, S. Jeon, D. S. Ko, I. S. Jung, J. H. Kim, K. Ito, Y. Kubo, K. Takei, S. Saito, and Y. H. Cho, *et al.*, Evolving affinity between coulombic reversibility and hysteretic phase transformations in nano-structured Silicon-based Lithium-ion Batteries, *Nat. Commun.* **9**, 479 (2018).  
 [3] T. Taniguchi, H. Sugiyama, H. Uekusa, M. Shiro, T. Asahi, and H. Koshima, Walking and rolling of crystals induced thermally by phase transition, *Nat. Commun.* **9**, 538 (2018).  
 [4] D. A. Rehn, Y. Li, E. Pop, and E. J. Reed, Theoretical potential for low energy consumption phase change memory utilizing electrostatically-induced structural phase

transitions in 2D materials, *NPJ Comput. Mater.* **4**, 2 (2018).  
 [5] M. W. Pin, E. J. Park, S. Choi, Y. I. Kim, C. H. Jeon, T. H. Ha, and Y. H. Kim, Atomistic evolution during the phase transition on a metastable single  $\text{NaYF}_4:\text{Yb,Er}$  upconversion nanoparticle, *Sci. Rep.* **8**, 2199 (2018).  
 [6] K. Muramoto, Y. Takahashi, N. Terakado, Y. Yamazaki, S. Suzuki, and T. Fujiwara,  $\text{VO}_2$ -dispersed glass: A new class of phase change material, *Sci. Rep.* **8**, 2275 (2018).  
 [7] G. G. D. Han, H. Li, and J. C. Grossman, Optically-controlled long-term storage and release of thermal energy in phase-change materials, *Nat. Commun.* **8**, 1446 (2017).  
 [8] J. Xue, C. Zhu, J. Li, H. Li, and Y. Xia, Integration of phase-change materials with electrospun fibers for promoting neurite outgrowth under controlled release, *Adv. Funct. Mater.* **28**, 1705563 (2018).  
 [9] S. Raoux, W. Wenig, and D. Ielmini, Phase change materials and their application to nonvolatile memories, *Chem. Rev.* **110**, 240 (2010).  
 [10] T. Wei, J. Wei, K. Zhang, H. Zhao, and L. Zhang, Grayscale image recording on  $\text{Ge}_2\text{Sb}_2\text{Te}_5$  thin films through laser-induced structural evolution, *Sci. Rep.* **7**, 42712 (2017).  
 [11] P. Hosseini, C. D. Wright, and H. Bhaskaran, An optoelectronic framework enabled by low-dimensional phase-change films, *Nature* **511**, 206 (2014).  
 [12] P. Singh, A. P. Singh, N. Kanda, M. Mishra, G. Gupta, and A. Thakur, High transmittance contrast in amorphous to hexagonal phase of  $\text{Ge}_2\text{Sb}_2\text{Te}_5$ : Reversible NIR-window, *Appl. Phys. Lett.* **111**, 261102 (2017).  
 [13] M. Wuttig and N. Yamada, Phase-change materials for rewriteable data storage, *Nat. Mater.* **6**, 824 (2007).  
 [14] M. L. Lee, K. T. Yong, C. L. Gan, L. H. Ting, S. B. M. Daud, and L. P. Shi, Crystallization and thermal stability of Sn-doped  $\text{Ge}_2\text{Sb}_2\text{Te}_5$  phase change material, *J. Phys. D Appl. Phys.* **41**, 215402 (2008).  
 [15] Sung-Jin Park, In-Soo Kim, Sang-Kyun Kim, Sung-Min Yoon, Byoung-Gon Yu, and Se-Young Choi, Phase transition characteristics and device performance of Si-doped  $\text{Ge}_2\text{Sb}_2\text{Te}_5$ , *Semicond. Sci. Tech.* **23**, 105006 (2008).  
 [16] X. Zhou, M. Xia, F. Rao, L. Wu, X. Li, Z. Song, S. Feng, and H. Sun, Understanding phase-change behaviors of carbon-doped  $\text{Ge}_2\text{Sb}_2\text{Te}_5$  for phase-change memory application, *ACS Appl. Mater. Interfaces* **6**, 14207 (2014).  
 [17] J. H. Han, Kwang-Sik Jeong, M. Ahn, Dong-Hyeok Lim, Won J. Yang, S. J. Park, and Mann-Ho Cho, Modulation of phase change characteristics in Ag-incorporated  $\text{Ge}_2\text{Sb}_2\text{Te}_5$  owing to changes in structural distortion and bond strength, *J. Mater. Chem. C* **5**, 3973 (2017).  
 [18] B. Prasai, G. Chen, and D. A. Drabold, Direct ab-initio molecular dynamic study of ultrafast phase change in Ag-alloyed  $\text{Ge}_2\text{Sb}_2\text{Te}_5$ , *Appl. Phys. Lett.* **102**, 041907 (2013).  
 [19] Ki-Ho Song, Sung-Won Kim, Jae-Hee Seo, and Hyun-Yong Lee, Characteristics of amorphous  $\text{Ag}_{0.1}(\text{Ge}_2\text{Sb}_2\text{Te}_5)_{0.9}$  thin film and its ultrafast crystallization, *J. Appl. Phys.* **104**, 103516 (2008).  
 [20] Chao-Te Lie, Po-Cheng Kuo, Wei-Chih Hsu, Ting-Hao Wu, Po-Wei Chen, and Sheng-Chi Chen,  $\text{Ge}_2\text{Sb}_2\text{Te}_5$  thin film doped with silver, *Jap. J. Appl. Phys.* **42**, 1026 (2003).  
 [21] Jae-Hee Seo, Ki-Ho Song, and Hyun-Yong Lee, Crystallization behavior of amorphous  $\text{Al}_x(\text{Ge}_2\text{Sb}_2\text{Te}_5)_{1-x}$  thin films, *J. Appl. Phys.* **108**, 064515 (2010).

- [22] T. H. Jeong, M. R. Kim, H. Seo, J. W. Park, and C. Yeon, Crystal structure and microstructure of nitrogen-doped  $\text{Ge}_2\text{Sb}_2\text{Te}_5$  thin film, *Jap. J. Appl. Phys.* **39**, 2775 (2000).
- [23] S. M. Kim, M. J. Shin, D. J. Choi, K. N. Lee, S. K. Hong, and Y. J. Park, Electrical properties and crystal structures of nitrogen-doped  $\text{Ge}_2\text{Sb}_2\text{Te}_5$  thin film for phase change memory, *Thin Solid Films* **469**, 322 (2004).
- [24] B. Liu, T. Zhang, J. Xia, Z. Song, S. Feng, and B. Chen, Nitrogen-implanted  $\text{Ge}_2\text{Sb}_2\text{Te}_5$  film used as multilevel storage media for phase change random access memory, *Semicond. Sci. Tech.* **19**, L61 (2004).
- [25] Il-Mok Park, Jung-Kyu Jung, Tae-Youl Yang, M. S. Yeom, Y. T. Kim, and Young-Chang Joo, Effect of Nitrogen implantation with low dose on thermomechanical properties and microstructure of  $\text{Ge}_2\text{Sb}_2\text{Te}_5$  films, *Jap. J. Appl. Phys.* **47**, 1491 (2008).
- [26] M. H. Jang, S. J. Park, D. H. Lim, M. H. Cho, K. H. Do, D. H. Ko, and H. C. Sohn, Phase change behavior in oxygen-incorporated  $\text{Ge}_2\text{Sb}_2\text{Te}_5$  films, *Appl. Phys. Lett.* **95**, 012102 (2009).
- [27] E. M. Vinod, K. Ramesh, and K. S. Sangunni, Structural transition and enhanced phase transition properties of Se doped  $\text{Ge}_2\text{Sb}_2\text{Te}_5$  alloys, *Sci. Rep.* **5**, 8050 (2015).
- [28] P. Singh, P. Sharma, V. Sharma, and A. Thakur, Linear and non-linear optical properties of Ag-doped  $\text{Ge}_2\text{Sb}_2\text{Te}_5$  thin films estimated by single transmission spectra, *Semicond. Sci. Tech.* **32**, 045015 (2017).
- [29] I. Friedrich, V. Weidenhof, W. Njoroge, P. Franz, and M. Wuttig, Structural transformations of  $\text{Ge}_2\text{Sb}_2\text{Te}_5$  films studied by electrical resistance measurements, *J. Appl. Phys.* **87**, 4130 (2000).
- [30] A. M. Galvan and J. G. Hernandez, Drude-like behavior of Ge:Sb:Te alloys in the infrared, *J. Appl. Phys.* **87**, 760 (2000).
- [31] E. M. Vinod, K. Ramesh, R. Ganesan, and K. S. Sangunni, Direct hexagonal transition of amorphous  $(\text{Ge}_2\text{Sb}_2\text{Te}_5)_{0.9}\text{Se}_{0.1}$  thin films, *Appl. Phys. Lett.* **104**, 063505 (2014).
- [32] Z. Sun, J. Zhou, and R. Ahuja, Structure of Phase Change Materials for Data Storage, *Phys. Rev. Lett.* **96**, 055507 (2006).
- [33] T. Matsunaga, N. Yamada, and Y. Kubota, Structures of stable and metastable  $\text{Ge}_2\text{Sb}_2\text{Te}_5$ , an intermetallic compound in GeTe– $\text{Sb}_2\text{Te}_3$  pseudobinary systems, *Acta Cryst. B* **60**, 685 (2004).
- [34] D. Loke, T. H. Lee, W. J. Wang, L. P. Shi, R. Zhao, Y. C. Yeo, T. C. Chong, and S. R. Elliott, Breaking the speed limits of phase-change memory, *Science* **336**, 1566 (2012).
- [35] F. Rao, K. Ding, Y. Zhou, Y. Zheng, M. Xia, S. Lv, Z. Song, S. Feng, I. Ronneberger, R. Mazzarello, *et al.*, Reducing the stochasticity of crystal nucleation to enable subnanosecond memory writing, *Science* **358**, 1423 (2017).
- [36] T. Siegrist, P. Jost, H. Volker, M. Woda, P. Merkelbach, C. Schlockermann, and M. Wuttig, Disorder-induced localization in crystalline phase-change materials, *Nat. Mater.* **10**, 202 (2011).
- [37] W. Zhang, A. Thiess, P. Zalden, R. Zeller, P. H. Dederichs, Jean-Yves Raty, M. Wuttig, S. Blügel, and R. Mazzarello, Role of vacancies in metal–insulator transitions of crystalline phase-change materials, *Nat. Mater.* **11**, 952 (2012).
- [38] B. Zhang, W. Zhang, Z. Shen, Y. Chen, J. Li, S. Zhang, Z. Zhang, M. Wuttig, R. Mazzarello, E. Ma, *et al.*, Element-resolved atomic structure imaging of rocksalt  $\text{Ge}_2\text{Sb}_2\text{Te}_5$  phase-change material, *Appl. Phys. Lett.* **108**, 191902 (2016).
- [39] P. Singh, R. Kaur, P. Sharma, V. Sharma, M. Mishra, G. Gupta, and A. Thakur, Optical band gap tuning of Ag doped  $\text{Ge}_2\text{Sb}_2\text{Te}_5$  thin films, *J. Mater. Sci.: Mater. Electron.* **28**, 11300 (2017).
- [40] K. Shportko, S. Kremers, M. Woda, D. Lencer, J. Robertson, and M. Wuttig, Resonant bonding in crystalline phase-change materials, *Nat. Mater.* **7**, 653 (2008).
- [41] J. Sanghera and D. Gibson, in *Chalcogenide Glasses* (Elsevier, 2014), p. 113.
- [42] Jiang-Jing Wang, Ya-Zhi Xu, R. Mazzarello, M. Wuttig, and W. Zhang, A review on disorder-driven metal–insulator transition in crystalline vacancy-rich GeSbTe phase-change materials, *Materials* **10**, 862 (2017).
- [43] X. Sun, M. Ehrhardt, A. Lotnyk, P. Lorenz, E. Thelander, J. W. Gerlach, T. Smausz, U. Decker, and B. Rauschenbach, Crystallization of  $\text{Ge}_2\text{Sb}_2\text{Te}_5$  thin films by nano- and femtosecond single laser pulse irradiation, *Sci. Rep.* **6**, 28246 (2016).
- [44] E. S. P. Leong, Y. J. Liu, B. Wang, and J. Teng, Effect of surface morphology on the optical properties in metal-dielectric-metal thin film systems, *ACS Appl. Mater. Interfaces* **3**, 1148 (2011).
- [45] Y. Yin, D. Niida, K. Ota, H. Sone, and S. Hosaka, Scanning electron microscope for in situ study of crystallization of  $\text{Ge}_2\text{Sb}_2\text{Te}_5$  in phase-change memory, *Rev. Sci. Instrum.* **78**, 126101 (2007).
- [46] Jung-Jin Kim, K. Kobayashi, E. Ikenaga, M. Kobata, S. Ueda, T. Matsunaga, K. Kifune, R. Kojima, and N. Yamada, Electronic structure of amorphous and crystalline  $(\text{GeTe})_{1-x}(\text{Sb}_2\text{Te}_3)_x$  investigated using hard x-ray photoemission spectroscopy, *Phys. Rev. B* **76**, 115124 (2007).
- [47] A. Klein, H. Dieker, B. Späth, P. Fons, A. Kolobov, C. Steimer, and M. Wuttig, Changes in Electronic Structure and Chemical Bonding Upon Crystallization of the Phase Change Material  $\text{GeSb}_2\text{Te}_4$ , *Phys. Rev. Lett.* **100**, 016402 (2008).